Arabian Journal of Chemistry (2023) **16**, 104705

King Saud University

Arabian Journal of Chemistry

www.ksu.edu.sa
www.sciencedirect.com

ORIGINAL ARTICLE

High antimicrobial, cytotoxicity, and catalytic activities of biosynthesized selenium nanoparticles using *Crocus caspius* extract

Seyedeh Roya Alizadeh [a], Mahdi Abbastabar [b], Mohsen Nosratabadi [b], Mohammad Ali Ebrahimzadeh [a,*]

[a] *Department of Medicinal Chemistry, School of Pharmacy and Pharmaceutical Sciences Research Center, Mazandaran University of Medical Sciences, Sari, Iran*
[b] *Department of Medical Mycology, School of Medicine, Mazandaran University of Medical Sciences, Sari, Iran*

Received 29 November 2022; accepted 20 February 2023
Available online 25 February 2023

KEYWORDS

Green selenium nanoparticles;
Antifungal;
Antibacterial;
Anticancer;
Dye degradation activities

Abstract The green method for synthesizing various nanoparticles is defined as one of the environmentally friendly, promising, and safer technologies. In our study, the selenium nanoparticles (C@SeNPs) were synthesized by *Crocus caspius* aqueous extract. The existence of functional groups involved in the synthesis of SeNPs that were connected with bioactive compounds was confirmed by the FT-IR spectrum. The TGA curve confirmed about 60 % weight loss between 260 and 500 °C, implying biomolecules surround the metallic core. XRD analysis displayed the trigonal nature of SeNPs. The SEM and TEM images of C@SeNPs demonstrated semi-spherical in shape. EDX analysis identified the intense bond of selenium. Biosynthesized C@SeNPs were discovered to have considerable antioxidant and antibacterial activities on several strains of bacteria. An IC_{50} value of 67.63 ± 2.5 µg/ml was obtained for their iron-chelating activity. In addition, the fabricated SeNPs have a strong growth inhibitory effect on MCF-7 and AGS cancer cells. C@SeNPs exhibited effective antifungal activity against tested fungi strains and antileishmanial activity against promastigotes. Besides, our NPs were able efficiently to degrade methylene blue (MB) dye in the presence of $NaBH_4$. Thus, the current findings suggest the benefits of using green technology to synthesize SeNPs with potential activity.

* Corresponding author.
E-mail address: MA.Ebrahimzadeh@mazums.ac.ir (M.A. Ebrahimzadeh).

Peer review under responsibility of King Saud University.

Production and hosting by Elsevier

https://doi.org/10.1016/j.arabjc.2023.104705
1878-5352

1. Introduction

Cancer, as one of the most challengeable issues of human society, globally has also been causing a growing economic burden on the cost of the health sector of the governments. Numerous progressive studies published up to now appear quite promising; however, they are yet to be fully established as a remedial or preventive action for cancer management. Since the emergence of the revolutionizing aspects of the nano-drug deliveries, compared with the hurdles facing traditional chemotherapeutic treatments in the last decades (such as side effects, drug resistance, etc.), the outstanding exertions given to overcome the cancers have been accelerated, which are especially directed toward the synthesizing nanostructured biomedical materials (Anu et al., 2020; Salem et al., 2021; Vahidi et al., 2020).

Selenium nanoparticles (SeNPs) have drawn a great deal of attention in the field of anticancer medication agents and drug carriers due to their unique chemopreventive effect and antitumor activity. In other words, it has been proved that the presence of Se in blood plasma, at low concentrations, would be effective in the inhibition of the cancer cell growth and neutralization of the malignancy (Menon et al., 2020). The detailed mechanism of the anticancer activity of Se is a matter of contention. However, acceptance of cell apoptosis has been suggested as the main mechanism behind the tumor chemoprevention of the selenium compounds (Menon et al., 2018). Thanks to the selectivity of the selenium, it is expected that the reactive oxygen species (ROS) would be increased in peritoneal cancer cells, while the normal cells were left intact at the same time (Vickers, 2017). Particle size, dose, and chemical form are the main factors, which determine the antitumorogenic effect of SeNPs. It is worthy to note that the preparation of Se in nano-dimension was shown to be significantly effective in reducing the risk of toxicity (Menon et al., 2018).

The conventional chemical and physical procedures applied for synthesizing the nanoparticles suffer from the toxicity of the chemical substances, which hinder their medical application. Green nanotechnology, given its safe procedure, simplicity, and low cost, is regarded as an epoch-making event in the potential antimicrobial agent and anticarcinogenic applications (Hassanien et al., 2019; Shirzadi-Ahodashti et al., 2022). To date, different green sources, namely microorganisms, enzymes, fungi, and plant extracts, have been applied for the biological synthesis process (Alizadeh and Ebrahimzadeh, 2020; Anu et al., 2017; Salem et al., 2021). Evaluating the anticancer activity of SeNPs on the three types of human cancers, Hassanien et al. have recently reported a plant-mediated procedure using *M. Oleifera* leave extract (Hassanien et al., 2019). Chitosan, a natural polymer, has been utilized as a stabilizing agent to synthesize SeNPs posing antibacterial activities (Boroumand et al., 2019). Anu et al. have also introduced a green method to prepare spherical nano-sized Se particles capped with garlic extract metabolites (Anu et al., 2017). By and large, it is believed that three main criteria, i.e., the solvent, the reducing agent, and the capping agent are of noticeable importance in the functionality of the NPs prepared via green chemistry. Therefore, optimizing a natural reducing and capping agent is vital in achieving stabilized and fine-sized nanoparticles (Vekariya et al., 2012). For example, the ascorbic acid, which abundantly exists in the *M. oleifera* leaves, is suspected to be responsible for reducing selenium ions (Se^{4+} to Se^{0}) (Hassanien et al., 2019). Several advantages have been reported for the biogenic SeNPs, which include (but are not limited to): suppressing the growth of small tumors, not aggregating with time while coming in conjugation with organic molecules and drugs, potent antimicrobial performance against pathogenic bacteria, antifungal activity, and sequester reduced mercury from polluted water, etc (Wadhwani et al., 2016).

Being aware of the usefulness of SeNPs in the antibacterial nanocoatings, some researchers put their efforts toward exploring their antibacterial activities. Spherical SeNPs with the size ~ 79 nm have functionally shown bacteriostatic effect against some foodborne pathogens (Nguyen et al., 2017). Furthermore, it has been well-known that the high surface area to volume ratio of SeNPs would significantly contribute to the antibacterial effect (Menon et al., 2020). The whole process is anticipated to be triggered by permeation through the cell membrane via endocytosis (Wadhwani et al., 2016).

One chore of the current research on the green-synthesized SeNPs has been the study of the degradation of organic dye pollutants for the water contamination treatment (Hassanien et al., 2019). The great advantage of using biosynthesized selenium nanoparticles is that they do not impart further waste or pollution to the environment. The study results on the effect of SeNPs on the dye of Congo red have demonstrated that the size of the SeNPs would be of crucial parameters on the photocatalytic activity (Yang et al., 2008). Recently, Tripathi et al. have shown that the SeNPs prepared by using a plant extract called *Ficus benghalensis* could effectively degrade the methylene blue in excess of about 57 % after 40 min of UV irradiation (Tripathi et al., 2020).

Among the biological substances for synthesizing SeNPs, plant extracts are highly demanded due to their availability and diversity (Hassanien et al., 2019). Bearing this in mind, our motive is to introduce a plant-mediated synthesis method based on an endemic species of Caspian forest, namely *Crocus caspius* (Shokrzadeh et al., 2019). The encouraging results published by researchers have confirmed the antioxidant activity of the extract of *C. caspius,* which stems from the presence of the phenol and flavonoid content. Furthermore, it has been traditionally exploited in folk medicine (Asadi, 2016). Despite being capping agents, phenolic compounds are suspected to be responsible for reducing Se^{4+} (Hassanien et al., 2019). The substances mentioned above are well-known for their anticancer performance (Khalili et al., 2016).

One could vividly find out that the research publications on the biogenic C@SeNPs are limited. Hence, in search of a straightforward green process for synthesizing SeNPs, which will be stable and possess antibacterial and anticancer functions, we have investigated the role of the extract of *C. caspius* as a reducing agent. The plant-mediated SeNPs were characterized by "Scanning electron microscope (SEM), Transmission electron microscope (TEM), X-ray diffraction (XRD), Energy dispersive X-ray analysis (EDX), Fourier transform infrared (FT-IR), Thermogravimetric and Differential thermal analysis (TG/DTA), Dynamic light scattering (DLS), zeta potential, and UV–vis techniques". The cell viability in the presence of C@SeNPs through the "Human gastric cancer cell line (AGS) and Human breast adenocarcinoma cell line (MCF-7)" was tested. In addition, selected gram-positive and -negative bacterial strains were examined to investigate the antibacterial efficiency of C@SeNPs. Furthermore, the evaluation of the antioxidant activity, antifungal, antileishmanial activities, and iron chelation ability of bio-synthesized C@SeNPs was conducted. Besides, the catalytic effect of C@SeNPs in the degradation of MB was analyzed in the presence of $NaBH_4$ and visible light.

2. Materials and methods

Sodium selenite, "3-(2-Pyridyl)-5,6-diphenyl-1,2,4-triazine-4′, 4″-disulfonic acid", "2,2-Diphenyl-1-picrylhydrazyl (DPPH)", and Sodium borohydride were provided from Sigma Aldrich (USA), Fluka, and Merck (Germany). Methylene blue and other chemicals were bought from Merck India ltd.

2.1. Synthesis of selenium nanoparticles (C@SeNPs) using C. caspius aqueous extract

The 10 g dried *C. caspius* was cut into smaller pieces and heated at 45–50 °C for 1 hr with 80 ml deionized water. Then, the flask was sonicated for 30 min. The obtained extract was filtered by filter paper (Whatman No. 1) and the filtrate was used to prepare selenium nanoparticles.

For the biosynthesis of SeNPs using *C. caspius* extract, Na_2SeO_3 (17.3 mg) dissolved in 10 ml deionized water was

shaken at 45–50 °C and 500 rpm, and then, *C. caspius* extract (5 ml) was added into the mixture. The reaction color changed from colorless to red or reddish-orange after 2 days, indicating that the Se ions had been reduced.

2.2. High-pressure liquid chromatography (HPLC)

UV–Vis spectrophotometric detector (model K-2600) and solvent delivery system with Rheodyne injection valve (20 µl sample loop) were used in the HPLC system. To elute the sample, an isocratic solvent system with acetonitrile: water: formic acid (17:82.6:0.4) mobile phase was employed with a flow rate of 1 ml/min and a run time of 40 min at 25 °C via an "ODS-C18 column (Shim-pack VP-ODS: 250 mm × 4.6 mm id, 5 mm)". Detection was also done with a UV–Vis detector (280 nm). The current technique was utilized to determine the phenol and flavonoid content of *C. caspius* extract.

2.3. Characterization of green synthesized C@SeNPs

The synthesized C@SeNPs were analyzed using UV–Visible spectroscopy "T80 UV–Vis spectrophotometer PGI, Beijing, China" in 200–800 nm. The surface morphology of C@SeNPs was detected by SEM ("TESCAN BRNO-Mira3 LMU") and their elemental composition was identified by EDX. Transmission electron microscopes (TEM) analysis ("TEM Philips EM 208S") exhibited the exact morphology of the synthesized SeNPs. The nature of C@SeNPs was defined by X-ray diffraction (XRD) under "PANalytical X-PERT PRO diffractometer ($2\theta = 10°$ to 80°) with Cu Kα (1.54 °A) source". The average size of C@SeNPs was measured by Scherrer's formula $D = 0.9\lambda/\beta\cos\theta$ (Shirmehenji et al., 2020). The functional groups involved in SeNPs synthesis were studied by FT-IR analysis. The FT-IR spectrum was recorded by "ATR, Agilent, Cary 630, FT-IR Spectrometer, equipment in 4000 and 650 cm^{-1}". The size and distribution of the C@SeNPs were determined using the DLS particle size analyzer ("Horiba-SZ-100-Z"). The thermal stability of the biosynthesized SeNPs was assessed by TGA and DTA (55–900 °C) at a heating rate of 0.01–100 K/min an autonomic TG/DTA ("STA 503, BAHR, Germany").

2.4. DPPH assay ("2,2-diphenyl-1-picryl-hydrazyl-hydrate")

The free radical scavenging activity of C@SeNPs was evaluated using the stable DPPH radical (Ebrahimzadeh et al., 2010; Hashemi et al., 2020; Nabavi et al., 2013). Different quantities of C@SeNPs (17.06, 34.125, 68.25, 196.5, and 273 µg/ml) were added to 1 ml of DPPH methanolic solution (4 mg/100 ml MeOH) and shacked in the dark at 25 °C. As a conventional control, BHA was utilized. The absorbance was determined at 517 nm after 15 min. The sample concentration necessary to scavenge 50 % of DPPH free radicals is known as the IC_{50} value. The following formula (1) was used to determine the sample's ability to scavenge the DPPH radical:

$$Inhibition of DPPH(\%) = \frac{absorbance of control - absorbance of test sample}{absorbance of control} \times 100 \quad (1)$$

2.5. Iron chelation activity (Ferrozine assay)

We assessed the ability of the C@SeNPs to chelate Fe^{2+} ions according to our previous published (Ebrahimzadeh et al., 2008; Ebrahimzadeh et al., 2010; Eslami et al., 2016; Hashemi et al., 2020). The fabricated C@SeNPs (2.034–130.16 µg/ml) mixed with 3 ml of deionized water were added to a solution containing $FeCl_2$ (50 µl × 2 mM) and ferrozine (100 µl × 5 mM) and shaken dynamically for 10 min. The solution's absorbance was taken spectrophotometrically at 562 nm. The standard compound was EDTA. The inhibition percentage of ferrozine-Fe^{2+} complex formation was calculated by equation (2):

$$Inhibition of complex formation(\%) = \frac{absorbance of control - absorbance sample}{absorbance of control} \times 100 \quad (2)$$

2.6. Antibacterial activity

A micro-broth dilution method was used to test the antibacterial impact of C@SeNPs against "several American Type Culture Collection (ATCC) bacteria including, *Staphylococcus aureus*, *Enterococcus faecalis* (gram-positive bacteria), *Proteus mirabilis*, *Pseudomonas aeruginosa, Klebsiella pneumoniae*, *Acinetobacter baumannii*, and *Escherichia coli* (gram-negative bacteria)". For the micro-broth dilution tests based on (Chowdhury et al., 2016), Muller-Hinton broth (MHB,100 µl), prepared C@SeNPs (0.133–136.67 µg/ml), and the diluted bacterial suspension (100 µl, 0.5 McFarland turbidity standards) were supplemented to each well of the 96 well plate and incubated for 24 hrs at 37 °C. The MIC was determined as the lowest concentration of C@SeNPs that caused no observable bacterial growth. To determine the MBC, a nutrient agar plate was filled with 10 µl of MIC well and three concentrated wells, which were incubated for 24 hrs. The MBC of the prepared C@SeNPs was determined after 24 hrs based on the lowest concentration that displayed no bacterial growth on the Muller Hinton agar surface. Pure bacterial suspensions (without any C@SeNPs) and MHB (without any bacterial suspension) were studied as positive and negative controls, respectively. The reference antibiotic was ciprofloxacin. All experiments were carried out in safe conditions (Mortazavi-Derazkola et al., 2020).

2.7. Antileishmanial activity

Leishmania major promastigotes (MRHO/IR/75/ER) were grown in RPMI-1640 medium. They were mixed with "10 % fetal bovine serum (FBS) and 100 µg/ml streptomycin/ penicillin at 24 °C". The media comprising promastigotes was sub-cultured every 72 hrs (Akhtari et al., 2019; Faridnia et al., 2018). Serial dilutions of C@SeNPs were prepared at concentrations of 273.5–8.547 µg/ml in 100 µl of RPMI-1640 medium. Each well of plates received 100 µl of the promastigotes medium (1×10^5) and incubation was performed for 72 hrs at 24 °C. After 72 hrs, 10 µl of MTT solution (2.5 mg/5 ml PBS) was added to each well and incubated for 5 hrs at 37 °C and were centrifuged (3000 rpm, 5 min). After this,

obtained suspensions were dissolved in isopropyl alcohol. The absorbance of the microplate was measured by ELISA reader "Synergy H1 hybrid multi-model microplate reader (Biotek Instruments, Winooski, Vermont, NE, USA" at 492 nm. Negative controls were three untreated wells comprising the parasite. The positive controls, Amphotericin B exhibited an IC_{50} value of 28.7 µg/ml (Hashemi et al., 2021).

2.8. Anticancer activity

The effect of C@SeNPs on "human gastric cancer cell line (AGS) and human breast adenocarcinoma cell line (MCF-7) "was assessed by MTT assay according to our previous research (Hashemi et al., 2020). In the living cells, "3- (4,5-dimethylthiazol-2-yl) 2.5- diphenyltetrazolium bromide" (yellow dye) was reduced to formazan crystal (purple) that is related to the activity of mitochondrial enzymes. The cells ($6–10 \times 10^3$ cells/well) were placed in a 96-well and incubated for 24 hrs at 37 °C in a 5 % CO_2. Then, the medium was removed and 100 µl of C@SeNPs (1, 10, 25, 50, and 100 µg/ml) was added to each well. After 24 hrs incubation, the C@SeNPs were removed, and 20 µl of MTT solution (5 mg/ml PBS) was loaded to each well and incubated in the dark for 4 hrs under standard conditions. After 4 hrs, DMSO (100 µl) was added to each well to dissolve the formazan crystals, recording the absorbance of the solution at 570 nm by "Synergy H1 hybrid multi-model microplate reader (Biotek Instruments, Winooski, Vermont, NE, USA". The percent cells viability was calculated by equation (3) (Al Jahdaly et al., 2021; Hashemi et al., 2020; Hashemi et al., 2022). The same assay was conducted using fibroblast cell lines to investigate the cytotoxic effects of C@SeNPs on noncancer cells. The experiments were validated thrice.

$$Cellviability(\%) = \frac{Theopticaldensityofthesamplewell}{Theopticaldensityofcontrolwell} \times 100 \quad (3)$$

2.9. Antifungal activity

The MIC value was estimated by broth micro-dilution method as described in "method M27-A3 from the Clinical and Laboratory Standards Institute (CLSI) formerly NCCLS" [15]. In the process, 200 µl of C@SeNPs was loaded to the first well of the 96-well plate, then 100 µl of RPMI media was entered into the wells of 2 to12 at the 96-well plate. In the following, 100 µl of the first well was taken and added to the second well, then serially diluted, 100 µl of cell suspensions were added to each well and after 24 hrs for two *Candida albicans* strains ((*IFRC1873*) and (*IFRC1874*)), and 48 hrs for *Aspergillus fumigatus* (*IFRC 1649*), *Aspergillus fumigatus* (*IFRC 1505*), *Trichophyton mentagrophytes* (*FR1_22130*), *Trichophyton mentagrophytes* (*FR5_22130*), *Fusarium proliferatum* (IFRC 1871), *Fusarium equiseti* (*IFRC 1872*), observable growth of wells were examined and the MIC value was defined. The references antibiotic was Itraconazole.

2.10. Catalytic reduction of MB dye using C@SeNPs

Methylene blue (MB) degradation under visible light was used to test the catalytic activity of biosynthesized C@SeNPs. Fresh $NaBH_4$ (200 µl × 0.1 M) was mixed with 5.77 ml H_2O and 30 µl MB solution (10 mM) during the process. After that, the prepared solution was treated with 40, 50, and 60 µl of C@SeNPs solution (546.67 µg/ml). Absorbance measurements in the region of 200–800 nm were taken at various time intervals. At 665 nm, the maximum absorption of MB was recorded. The pseudo-first-order reaction (4) was used to follow the MB degradation rate; At and A0 were presented as the absorbance at interval times and time 0, respectively (Nadaf and Kanase, 2019).

$$Ln\left(\frac{At}{A0}\right) = -kt \quad (4)$$

2.11. Statistical analysis

The biological analysis was performed in triplicate. One-way analysis of variance (ANOVA) was accomplished, followed by Tukey's test using the GraphPad Prism 9.0 software. Statistical significance was defined as $p < 0.05$.

3. Results and discussions

3.1. Preparation and characterization of C@SeNPs

The color of the mixture solution comprising sodium selenite and *C. caspius* aqueous extract changed from light brown to red or reddish-orange after completing the SeNPs production reaction due to SPR of the produced SeNPs, indicating that Se ions were reduced into SeNPs using functional groups (natural reductants) in *C. caspius* extract (Hatami et al., 2020). Fig. 1 displays the red color of the solution with synthesized C@SeNPs after 48 hrs. Different pH levels (6 (extract pH), 10, 12) and temperatures (25–30, 45–50, 75–80 °C) were evaluated to optimize the synthesis condition of SeNPs using *C. caspius*; the results showed that the solution color was changed from colorless to red or reddish-orange at the 45–50 °C and extract pH (pH = 6); however, this color change did not occur in other conditions. In addition, UV–vis spectrophotometry was used to characterize C@SeNPs by reporting the absorption of colloidal solution at 200–800 nm (Fig. 1). Fardsadegh and coworkers effectively prepared SeNPs with a particle size of 136 nm using the leaf extract of *Pelargonium zonale* and microwave heating (Fardsadegh et al., 2019).

The size, shape, and distribution of C@SeNPs were investigated using the TEM image, as shown in Fig. 2a. C@SeNPs have a semi-spherical shape, and their average size is about 20.34 nm in the provided image. The image proved the fabrication of NPs that were capped with their biomoites. In addition, the SEM image (Fig. 2b) revealed a semi-spherical shape for the surface morphology of C@SeNPs with an average particle size of around 23.47 nm, which is very close to the TEM results. Furthermore, synthesized NPs possess a good polydispersity. The histogram from the SEM image demonstrated that about 90 % of the fabricated C@SeNPs possess a size range of 10–40 nm (Fig. 2c). Keskin et al. synthesized SeNPs using *Lysinibacillus* sp. NOSK and the SEM analysis showed a spherical shape around 130 nm (Keskin et al., 2020). In a study in 2019, according to the SEM data, the prepared SeNPs were spherical shape with a size range of approximately 100–150 nm (Menon et al., 2019).

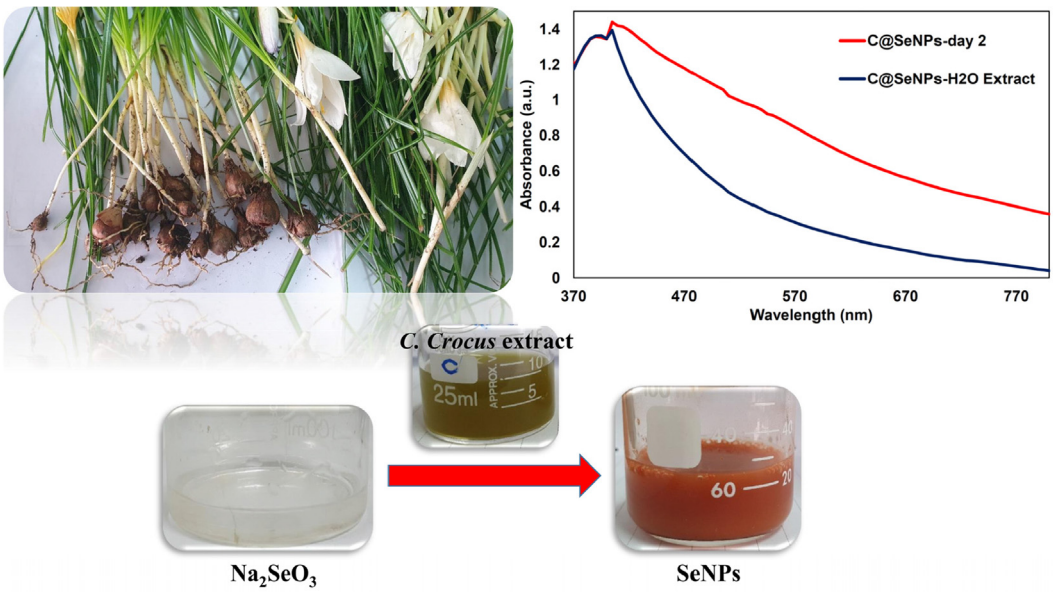

Fig. 1 The UV–vis spectra of synthesized SeNPs by *C. caspius* aqueous extract.

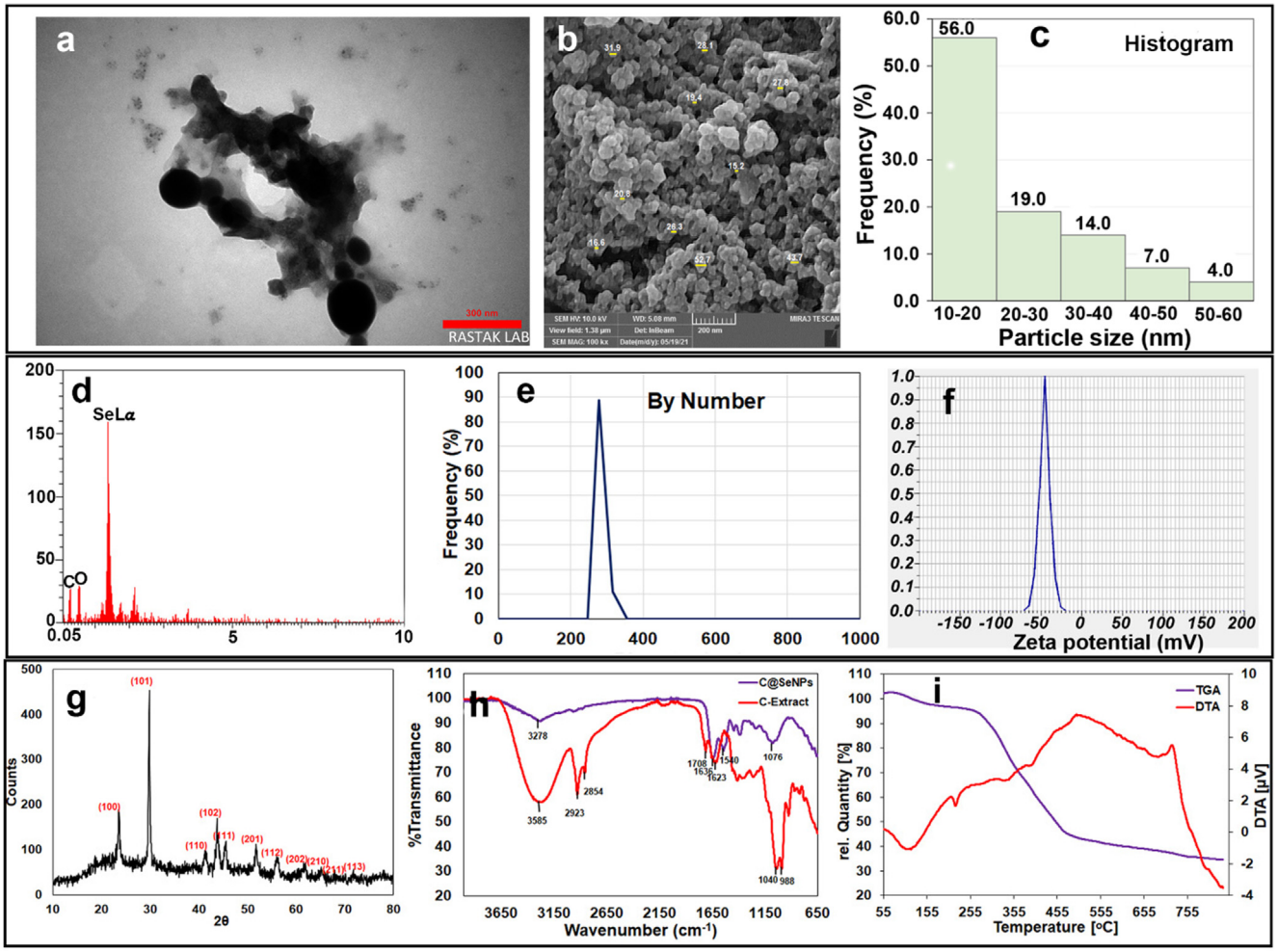

Fig. 2 A) the tem image with 20.34 nm average size with semi-spherical shape; b) the SEM image with 23.47 nm average size; c) the histogram obtained from SEM image; d) the EDX analysis containing C, O, and Se bonds; e) The DLS graph with 266.3 nm average size; f) zeta potential analysis with −44.75 mV; g) XRD data of green synthesized C@SeNPs; h) FT-IR graph of C@SeNPs and C-Extract; i) TG/DTA data of C@SeNPs.

EDX analysis of the extract-mediated SeNPs from the portion of SEM images has confirmed that the majority of the detected elements in the synthesized sample is Se (Fig. 2d). However, similar to what is reported in the literature, the presence of some amount of carbon and oxygen (and some other elements) might be inevitable, which stems from the natural substances (Tripathi et al., 2020). Keskin et al. displayed Se signal along with C and O group peaks using the elemental analysis (Alipour et al., 2021).

The size distribution of C@SeNPs was measured by DLS particle size analyzer, and the average size of the NPs was determined to be 266.3 nm by number (Fig. 2e); due to the aggregation of C@SeNPs in the solution, some of the large particles appeared in the DLS graph. The particle size distribution of ginger mediated-SeNPs was obtained in the range of 100–120 nm by Menon et al (Menon et al., 2019). The obtained size of C@SeNPs using two methods, zetasizer and TEM, differed; because TEM determines the actual particle radius while zetasizer determines the average hydrodynamic radius. In the green synthesis, the intrinsic capping provided an additional benefit of stability (Mittal et al., 2014).

The surface electric charge of the prepared C@SeNPs is defined by Zeta potential; the NPs stability in colloids possess a direct relationship with the ZP value (Hatami et al., 2020). The zeta potential of synthesized C@SeNPs was -44.75 ± 0.95 mV, indicating the nanoparticles were stable (Fig. 2f). Thus, the phytochemicals as capping agents can be induced repulsive forces on the surface of nanoparticles, making them more stable.

The XRD analysis is conducted to investigate the phase composition and crystalline nature of the plant-mediated SeNPs, which is presented in Fig. 2g. The result shows several Bragg's reflections at (100), (101), (110), (102), (111), (201), (112), (202), (210), (211), and (113) ascribing 23.61, 29.85, 41.36, 43.83, 45.52, 51.83, 56.20, 61.67, 65.11, 67.95, and 71.75 of trigonal selenium crystallographic planes (Menon et al., 2021). The green synthesis of SeNPs using *Withania somnifera, Emblica oficinalis*, and *Pseudomonas aeruginosa* (Amiri et al., 2021) was consistent with our study. The crystallite size is evaluated using the well-known Debye-Scherrer equation (Menon et al., 2020). The calculated crystallite size for our synthesized SeNPs is about 33.42 nm.

The FT-IR analysis is performed to explore the effect of the organic moieties corresponding to the *C. caspius*. In Fig. 2h, the spectrum of the extract is compared with that of plant-mediated NPs. The broad and rich hydroxyl band at 3585 cm^{-1} of C-Extract attests to this fact that there are plenty of phenolic compounds and flavones. The symmetric and antisymmetric stretching vibrational of C—H group are also observed at 2854 cm^{-1} and 2923 cm^{-1}, respectively (Boroumand et al., 2019). The 1708 cm^{-1} peak is evidence of the presence of carbonyl functional group in the C-Extract (Nasrollahzadeh and Sajadi, 2015). The C═O stretching feature, which appeared around 1636 cm^{-1} in the FT-IR of C@SeNPs, has shown a small shift toward higher wavenumbers in the case of C-Extract (Hamelian et al., 2018). Anu et al. have ascribed a similar observation to the formation of Se nanoparticles as a result of reduction of the carbonyl groups presented in the natural plant (Anu et al., 2020). The band at 1040 cm^{-1} is assigned to C—N stretching vibrations of aliphatic amines (Salem et al., 2021). The peak at lower wavenumbers is expected to be as a result of either ν(C—O) or ν (C—C) vibrations.

The above results testified the involvement of the functional groups such as OH, C═O, and C—H. This could be easily observed by the significant vanishing of the OH group in the case of FT-IR spectra of the plant-mediated SeNPs. Hence, the presented FT-IR has vividly identified the interaction between Se and metabolites of plant extract, which is responsible for capping and reducing intermediate for as-synthesized SeNPs.

TG/DTA curve obtained from C@SeNPs (Fig. 2i) confirmed about 60 % weight loss between 260 and 500 °C in TGA analysis, suggesting that biomolecules surround the metallic core (Nasrollahzadeh et al., 2016). At around 100 °C, no significant weight loss showed the lake or low content of moisture at the product. Furthermore, there was no considerable weight loss (about 5 %) at temperatures about 500–850 °C, indicating the stability of C@SeNPs.

In the DTA curve of C@SeNPs, one endothermic peak at about 110 °C is related to the loss of low content of water molecules (Elahi et al., 2020; Sabouri et al., 2019). One endothermic peak about 220 °C is related to the melting point of SeNPs (Ezhuthupurakkal et al., 2017), and two weak endothermic peaks around 350 and 400 may be responsible for the decomposition of organic biomolecules. An exothermic peak of about 720 possibly corresponds to the boiling point of Se.

3.2. HPLC analysis

The HPLC method was selected for the direct detection of phenolic acids in a *C.caspius* extract. In this investigation, it was obvious that phenolic acids and flavonoids in *C.caspius* extract could be separated using an isocratic solvent system. According to HPLC analysis, the main constituents existing in this extract are phenolic acid and flavonoid compounds, such as catechin, gallic acid, caffeic acid, *p*-coumaric acid, and rutin, (Table. 1). Fig. 3 is suggested as a mechanism for creating SeNPs in the presence of *C.caspius* extract. Based on the HPLC data, catechin (8.403 mg/g plant) was the major antioxidant among the other injected standards. Generally, the *ortho*-hydroxyl groups of these compounds are involved in the synthesis of SeNPs. Se^{4+} is reduced to Se^{0} when occurs releasing two electrons in the flavonoid ring. The catechol ring is oxidized into a 3′,4′-quinone ring as a stable end product. Se undergoes additional aggregation to larger clusters as the process progresses, eventually forming SeNPs. Quinone form of catechin is also linked to the surface of NPs, resulting in less Se^{0} aggregation at the nanoscale.

Table 1 The content of some phenolic acids in the *crocus caspius*.

Phenolic acid	Retention time (min)	*Crocus caspius* (mg/g)
Catechin	2.48	8.403
Gallic acid	3.58	0.14
p-Coumaric acid	9.76	0.107
Caffeic acid	17.28	0.027
Rutin	26.2	1.7

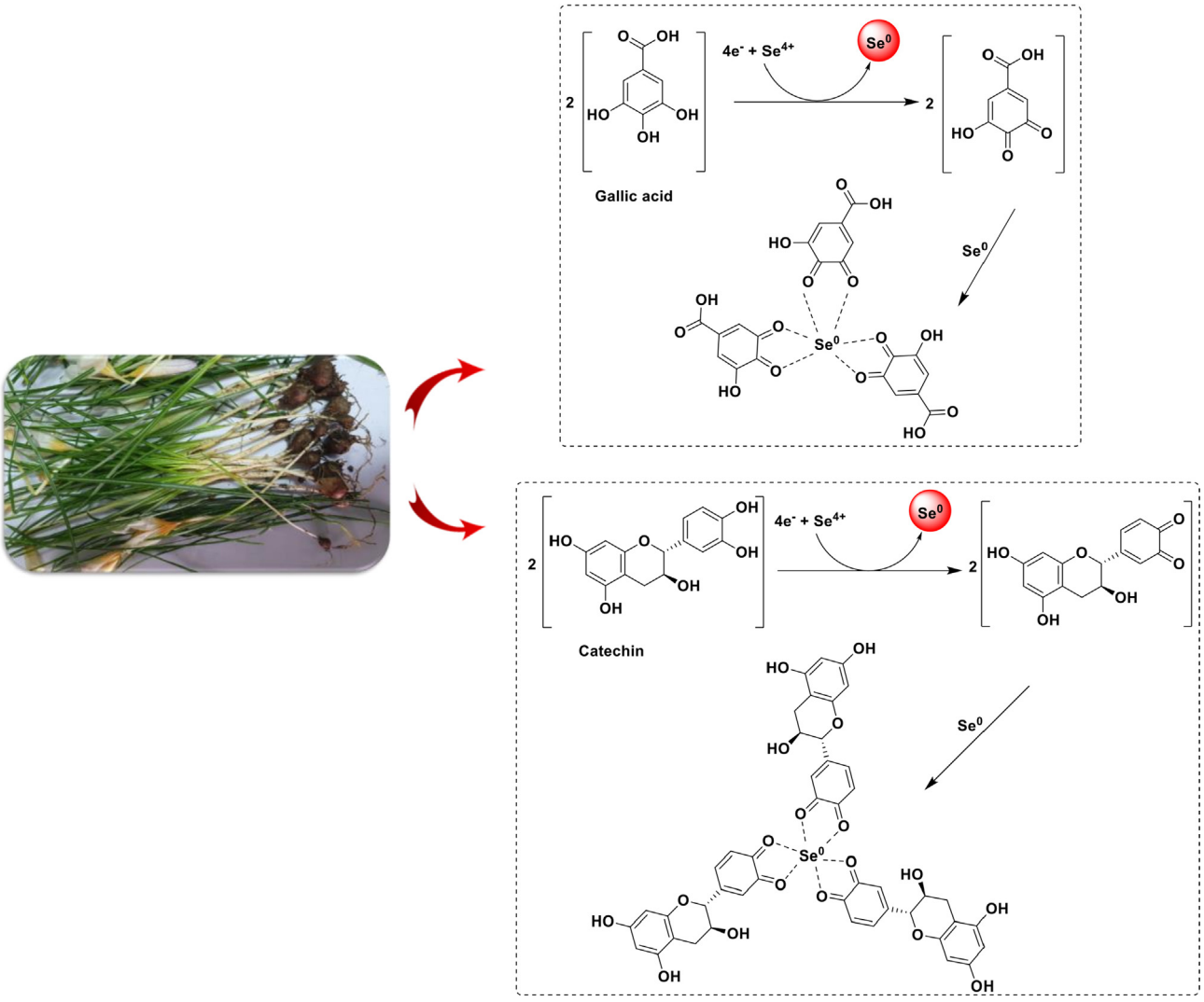

Fig. 3 The possible mechanism of the biosynthesized selenium nanoparticles using *Crocus caspius* extract.

3.3. DPPH assay

The DPPH assay is a quick and easy approach to evaluate a compound's capacity to quench free radicals (Nakkala et al., 2016). Due to the transfer of free electrons, when an antioxidant compound reacts with this reagent, the violet color of the solution converts to colorless, demonstrating that the antioxidant agent with hydrogen-donating activity has taken up the free radicals. In our study, the antioxidant activity of various concentrations of C@SeNPs (17.06–273 µg/ml) was investigated by DPPH assay. The absorbance was recorded by helping spectrophotometry. In this assay, the IC_{50} ("concentration required to inhibit 50 % of free radicals") of C@SeNPs has obtained 123.9 ± 2.5 µg/ml. The standard compound was Butylated Hydroxyanisole (BHA) with an IC_{50} value of 53.96 µg/ml. As a result, the antioxidant activity increased with increasing the concentration of the C@SeNPs. In a study (2019) was reported that ginger extract mediated-SeNPs with spherical shape and 100–150 nm presented an IC_{50} value of 125 µg/ml (Menon et al., 2019). In another investigation, biosynthesized SeNPs with 4–16 nm were shown to have an IC_{50} of 0.225 µg/ml (Kokila et al., 2017).

3.4. Metal chelating activity

The iron chelating activity of our synthesized C@SeNPs (2.0 34–130.16 µg/ml) was studied, and it was discovered that they could chelate ferrous (Fe^{2+}) ion. The IC_{50} value was determined by the concentration required to inhibit 50 % of the Ferrozine-Fe^{2+} complex was known as; C@SeNPs had an IC_{50} value of 67.63 ± 1.11 µg/ml. In addition, IC_{50} value for positive control (EDTA) was obtained 18.27 ± 0.59 µg/ml. Therefore, prepared C@SeNPs revealed remarkable iron chelation activity.

3.5. Antibacterial activity

Antibacterial potential of C@SeNPs green synthesized from *C. caspius* extract was assessed against the ATCC bacterial strains using micro-broth dilution method (Table. 2). The antibacterial potential of fabricated C@SeNPs exhibited remarkable antibacterial activity against all tested bacterial strains, according to the findings. Maximum antibacterial activity was seen against *S. aureus* and *A. baumannii* at a MIC value of 17.08 µg/ml, and MBCs of 273.33 and

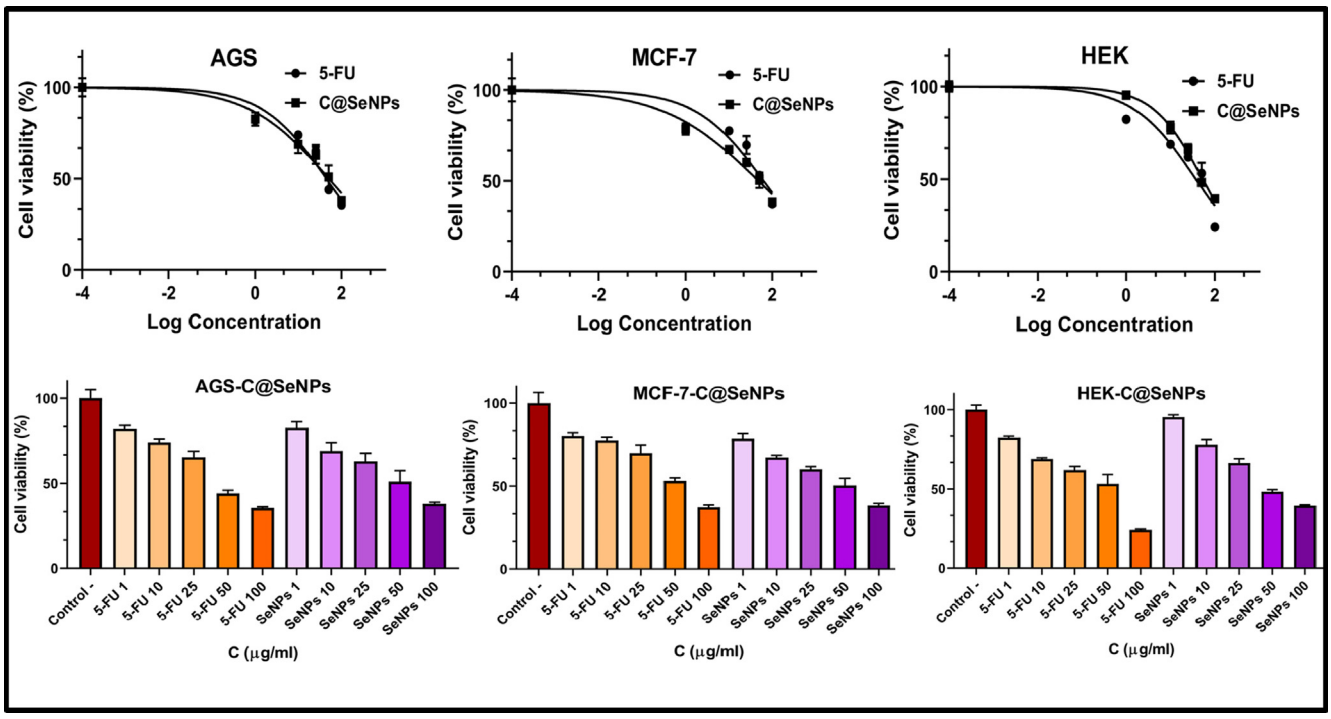

Fig. 4 Effect of biosynthesized C@SeNPs on viability of AGS, MCF-7, and HEK cells determined by MTT assays.

Table 2 The MIC and MBC values obtained from biosynthesized C@SeNPs against some bacterial strains.

Bacteria	ATCC	C@SeNPs		Extract	Ciprofloxacin
		MIC(μg/ml)	MBC(μg/ml)	MIC(μg/ml)	MIC(μg/ml)
S. aureus	ATCC 29,213	17.08	273.33	> 4000	0.21
E. faecalis	ATCC 29,212	136.66	546.67	> 4000	0.21
P. aeruginosa	ATCC 27,853	34.17	273.33	> 4000	0.3
A. baumannii	ATCC 19,606	17.08	68.33	> 4000	0.25
E. coli	ATCC 25,922	68.33	1093.34	> 4000	0.1
K. pneumoniae	ATCC 700,603	68.33	1093.34	> 4000	0.1
P. mirabilis	ATCC 25,933	136.66	273.33	> 4000	0.1

68.33 μg/ml. Synthesized C@SeNPs also exhibited moderate activity against *P. aeruginosa, E. coli,* and *K. pneumoniae* with MICs of 34.17, 68.33, and 68.33 μg/ml. In addition, *E. faecalis* and *Proteus mirabilis* presented MIC of 136.66 μg/ml. The SeNPs biosynthesized by *bee propolis* ethanol extract revealed antimicrobial and antioxidant potential (Shubharani et al., 2019). An efficient antimicrobial activity was reported for the SeNPs synthesized using *Allium sativum* extract against *S. aureus* and *B. subtilis* (Jay and Shafkat, 2018). *Diospyros montana* mediated-SeNPs display potent antimicrobial activity against *S. aureus*, *E. coli*, and *A. niger* (Kokila et al., 2017). Therefore, our prepared SeNPs can be considered as an effective antibacterial agent.

3.6. Anticancer activity against MCF-7 and AGS cell lines

The *in vitro* cytotoxic effects of biosynthesized C@SeNPs were checked on two cancer cell lines, MCF-7 and AGS, and normal cell (HEK) using the MTT assay (Fig. 4). Based on the result, the growth of cells decreased with increasing the content of C@SeNPs. Synthesized selenium nanoparticles exhibited capacity to limit the growth of AGS and MCF-7 cell lines by 18 % and 22 % at lowest concentration (1 μg/ml). The IC_{50} values of 47.59, 50.7, and 53.33 μg/ml were found on MCF-7, AGS, and HEK cells, respectively. Besides, 5-FU as standard anticancer demonstrated IC_{50} values of 62.73, 44.25, and 37.39 μg/ml against MCF-7, AGS, and HEK cell lines, respectively. Therefore, C@SeNPs presented a strong growth inhibitory impact that was close to standard anticancer. SeNPs prepared by the biomolecules existing in *M. Oleifera* extract has revealed to be effective against MCF-7 cells, Caco-2 cells, and HepG2 cells with IC_{50} values of 252.44, 150.87, and 392.57 μg/ml (Hassanien et al., 2019). *Withania somnifera* leaves extract mediated-SeNPs indicated antiproliferative activity against A549 cells (IC_{50} = 25 μg/ml) (Alagesan and Venugopal, 2019). In another study, SeNPs produced using *Acinetobacter* displayed effective anticancer activity against "4T1, MCF-7 and NIH/3T3, HEK293" (Wadhwani et al., 2017). In various studies, potential anticancer mechanisms of SeNPs have all been proposed the formation of reactive

Table 3 The MIC value achieved from biosynthesized C@SeNPs against several fungi isolates.

Fungi isolates tasted	C@SeNPs	Extract	Itraconazole
	MIC (μg/ml)	MIC (μg/ml)	MIC (μg/ml)
Aspergillus fumigatus (IFRC1649)	0.53	> 2500	≥ 16
Aspergillus fumigatus (IFRC1505)	0.53	> 2500	≥ 16
Trichophyton mentagrophytes (FR1_22130)	0.53	> 2500	≥ 16
Trichophyton mentagrophytes (FR5_22130)	0.53	> 2500	≥ 16
Fusarium proliferatum (IFRC 1871)	0.53	> 2500	≥ 16
Fusarium equiseti (IFRC 1872)	0.53	> 2500	≥ 16
Candida albicans (IFRC1873)	0.53	> 2500	≥ 16
Candida albicans (IFRC1874)	0.53	> 2500	≥ 16

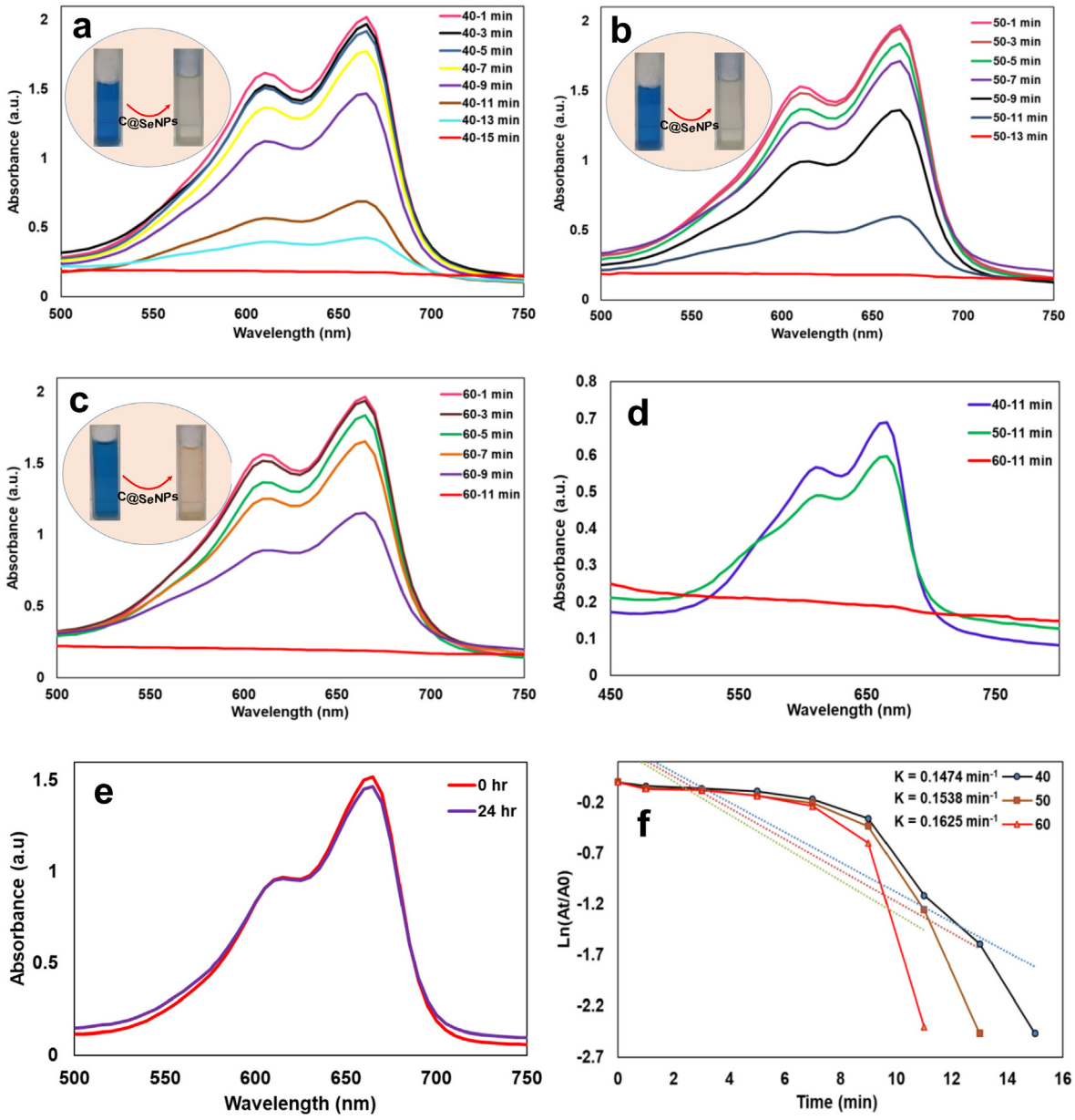

Fig. 5 a-c) UV–vis spectra of MB reduction reaction after adding 40, 50, and 60 μl C@SeNPs; d) the comparison of three volumes of C@SeNPs in the reduction of MB dye; e) reaction mixture without any nanocatalyst C@SeNPs until 24 hrs; f) reaction constant calculated for three reduction reactions.

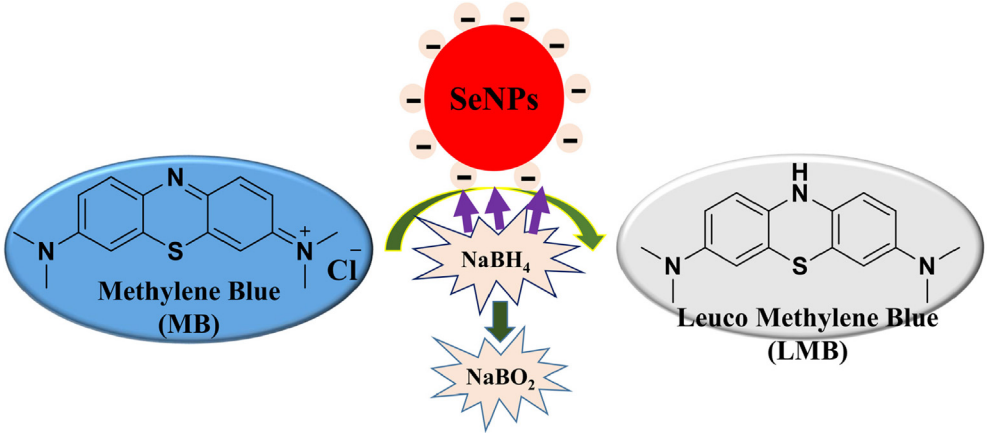

Fig. 6 The mechanism of action of biofabricated C@SeNPs in the reduction of methylene blue (MB) in the presence of $NaBH_4$.

oxygen species (ROS), the activation of apoptotic pathways, cellular homeostasis disruption, mitochondrial malfunction, cell cycle arrest, and DNA fragmentation (Vahidi et al., 2020).

3.7. Antileishmanial activity

Due to the importance of discovering antileishmanial drugs, fabricated C@SeNPs (8.547–273.5 µg/ml) were assessed for their antileishmanial activity (*in vitro*) and showed an IC_{50} value of 42.81 µg/ml. The amount of IC_{50} for amphotericin B (positive control) was obtained 28.7 µg/ml. In comparison, green synthesized C@SeNPs diplayed antileishmaniasis potency very close to positive control. Hence, our C@SeNPs can be discussed as promising antileishmanial agents. In the research by Mahmoudvand et al. was presented that SeNPs showed the IC_{50} values of 2.7 and 3.6 µg/ml against "sensitive and glucantime-resistant strains" (Mahmoudvand et al., 2014). In another study, SeNPs mediated *Bacillus* sp. MSh-1 demonstrated an IC_{50} of 1.62 ± 0.6 µg/ml against the promastigote (Beheshti et al., 2013). According to the researchers, DNA fragmentation could be the main mechanism of cellular apoptosis in promastigotes exposed to SeNPs (Ahmad et al., 2020).

3.8. Antifungal activity

The antifungal activity of fabricated C@SeNPs was evaluated by standard microdilution protocol. Based on the result, the C@SeNPs (273.5–0.27 µg/ml) inhibited the tested fungi strains, containing *Candida albicans* (*IFRC1873*), *Candida albicans* (*IFRC1874*), *Aspergillus fumigatus* (*IFRC 1649*), *Aspergillus fumigatus* (*IFRC 1505*), *Trichophyton mentagrophytes* (*FR1_22130*), *Trichophyton mentagrophytes* (*FR5_22130*), *Fusarium proliferatum* (IFRC 1871), and *Fusarium equiseti* (*IFRC 1872*), with low MIC values (Table. 3). C@SeNPs exhibited MIC values of 0.53 µg/ml against all tested strains. The MIC of the reference antibiotic (Itraconazole) was found around 16 µg/ml that was higher than C@SeNPs (0.53 µg/ml). In addition, the two tested *C. albicans* were fully resistance against fluconazole with an MIC value of around 64 µg/ml. Shakibaie and coworkers found MIC values of 70 µg/ml and 100 µg/ml for the biosynthesized SeNPs by *Bacillus species Msh-1* against *C. albicans* and *A. fumigatus* (Shakibaie et al., 2015). *Bacillus megaterium*-Mediated SeNPs showed antifungal activity against *Rhizoctonia solani* with minimum inhibition of 0.0625 mM (Hashem et al., 2021). As a result, our synthesized C@SeNPs can be considered as promising antifungal agents because of their strong inhibitory potential against several fungi strains.

Selenium has been discovered to promote the production of ROS; both elements are able to react with intracellular thiols and create intermediates that lead to oxidative stress by producing superoxide radicals. Nanoparticles can affect the integrity of cell membrane or wall and lead to their functional damages (Ismail et al., 2016).

3.9. Catalytic reduction of MB by C@SeNPs

Removing organic contaminants from industrial wastewaters is an essential part of environmental technology (Hassanien et al., 2019). This work was designed to study the reduction of MB dye using biosynthesized C@SeNPs (nanocatalyst) and $NaBH_4$ (reducing agent) (Fig. 5a-f). When dye reduction was tried without C@SeNPs, the procedure did not demonstrate any progress until after 24 hrs test period. The reduction could not be completed with $NaBH_4$; the absorbance peak at 665 nm remained unchanged, as seen in Fig. 5e. Therefore, 40, 50, and 60 µl of our SeNPs (546.67 µg/ml) was added to the MB and $NaBH_4$ solution (Fig. 5a-c). The disappearance of the solution was observed after 15, 13, and 11 min, respectively. The MB reduction time was shown to be faster when the concentration of NPs was increased (Fig. 5d). The reduction rate was obtained 0.1474, 0.1538, and 0.1625 min^{-1} for 40, 50, and 60 µl of C@SeNPs (Fig. 5f). Nanoparticles provide a larger surface area; therefore, the reduction rate increases after adding C@SeNPs to the solution (MB and $NaBH_4$). This data showed that the biosynthesized C@SeNPs indicated good catalytic activity in the reducing MB that the action mechanism represented in Fig. 6.

4. Conclusion

SeNPs can be employed for a variety of applications, including medicine, due to their therapeutic characteristics. The production of SeNPs through an aqueous extract of *C. caspius* was revealed using UV–vis spectra, XRD, EDX, FT-IR, SEM, TEM, TG/DTA, DLS, and zeta potential. Biomolecules found in *C. caspius* extracts were attributed

to reducing Se^{4+} to Se (0). The existence of functional groups involved in the synthesis of SeNPs that were connected with bioactive compounds was confirmed by the FT-IR spectrum. The TGA curve confirmed about 60 % weight loss between 260 and 500 °C, implying biomolecules surround the metallic core. The biofabricated SeNPs indicated a semi-spherical shape with a size of around 23.47 nm. The presence of C@SeNPs in the suspension solution is confirmed by UV analysis. The trigonal nature of SeNPs with a size of 33.42 nm was revealed by X-ray diffraction (XRD) research. The TEM analysis showed a semi-spherical shape with an average size of 20.34 nm that very close to the SEM data. The DLS particle size analyzer revealed an average size of 266.3 nm by number and zeta potential of −44.75 mV for C@SeNPs. The strong bond of selenium was discovered via EDX analysis. In the investigation of biological activity, C@SeNPs demonstrated potent radical scavenging activity with an IC_{50} value of 123.9 ± 2.5 μg/ml, and they showed considerable antibacterial activity against gram-positive and -negative bacterial strains. The iron-chelating activity of C@SeNPs was determined to have an IC_{50} value of 67.63 ± 2.5 μg/ml. In addition, the fabricated SeNPs effectively inhibited the growth of MCF-7 and AGS cancer cells (IC_{50} = 47.59 and 50.7 μg/ml). Our synthesized NPs demonstrated effective antifungal activity against several fungi strains (MIC = 0.5 3 μg/ml) and antileishmanial activity against promastigotes (IC_{50} = 42.81 μg/ml). Furthermore, C@SeNPs degraded methylene blue (MB) dye efficiently in the presence of $NaBH_4$. The current investigations point to the potential benefits of adopting green technology to synthesize SeNPs with activity.

CRediT authorship contribution statement

Seyedeh Roya Alizadeh: Conceptualization, Methodology, Formal analysis, Investigation, Writing – original draft. **Mahdi Abbastabar:** Methodology, Writing – original draft. **Mohsen Nosratabadi:** Methodology, Writing – original draft. **Mohammad Ali Ebrahimzadeh:** Conceptualization, Resources, Writing – original draft, Supervision.

Declaration of Competing Interest

The authors declare that they have no known competing financial interests or personal relationships that could have appeared to influence the work reported in this paper.

Acknowledgment

This study was conducted with the financial support of the Research Council of Mazandaran University of Medical Sciences, Iran (Grant No. 10555).

References

Ahmad, A., Ullah, S., Syed, F., Tahir, K., Khan, A.U., Yuan, Q., 2020. Biogenic metal nanoparticles as a potential class of antileishmanial agents: mechanisms and molecular targets. Nanomedicine 15 (08), 809–828. https://doi.org/10.2217/nnm-2019-0413.

Akhtari, J., Faridnia, R., Kalani, H., Bastani, R., Fakhar, M., Rezvan, H., Beydokhti, A.K., 2019. Potent in vitro antileishmanial activity of a nanoformulation of cisplatin with carbon nanotubes against Leishmania major. J. Glob. Antimicrob. Resist. 16, 11–16. https://doi.org/10.1016/j.jgar.2018.09.004.

Al Jahdaly, B.A., Al-Radadi, N.S., Eldin, G.M., Almahri, A., Ahmed, M., Shoueir, K., Janowska, I., 2021. Selenium nanoparticles synthesized using an eco-friendly method: dye decolorization from aqueous solutions, cell viability, antioxidant, and antibacterial effectiveness. J. Mater. Res. Technol. 11, 85–97. https://doi.org/10.1016/j.jmrt.2020.12.098.

Alagesan, V., Venugopal, S., 2019. Green synthesis of selenium nanoparticle using leaves extract of withania somnifera and its biological applications and photocatalytic activities. Bionanoscience 9 (1), 105–116. https://doi.org/10.1007/s12668-018-0566-8.

Alipour, S., Kalari, S., Morowvat, M.H., Sabahi, Z., Dehshahri, A., 2021. Green synthesis of selenium nanoparticles by Cyanobacterium Spirulina platensis (abdf2224): cultivation condition quality controls. Biomed Res. Int. 1–11. https://doi.org/10.1155/2021/6635297.

Alizadeh, S.R., Ebrahimzadeh, M.A., 2020. Characterization and anticancer activities of green synthesized CuO nanoparticles. a review. Anticancer Agents Med. Chem. 21, 1529–1543. https://doi.org/10.2174/1871520620666201029111532.

Amiri, H., Hashemy, S.I., Sabouri, Z., Javid, H., Darroudi, M., 2021. Green synthesized selenium nanoparticles for ovarian cancer cell apoptosis. Res. Chem. Intermed. 47 (6), 2539–2556. https://doi.org/10.1007/s11164-021-04424-8.

Anu, K., Singaravelu, G., Murugan, K., Benelli, G., 2017. Green-synthesis of selenium nanoparticles using garlic cloves (Allium sativum): biophysical characterization and cytotoxicity on vero cells. J Clust Sci. 28 (1), 551–563. https://doi.org/10.1007/s10876-016-1123-7.

Anu, K., Devanesan, S., Prasanth, R., AlSalhi, M.S., Ajithkumar, S., Singaravelu, G., 2020. Biogenesis of selenium nanoparticles and their anti-leukemia activity. J. King Saud Univ. Sci. 32 (4), 2520–2526. https://doi.org/10.1016/j.jksus.2020.04.018.

Asadi, M., 2016. Antioxidant and antimicrobial activities in the different extracts of Caspian saffron, Crocus caspius Fisch & CA Mey. ex Hohen. Casp. J. Environ. Sci. 14 (4), 331–338.

Beheshti, N., Soflaei, S., Shakibaie, M., Yazdi, M.H., Ghaffarifar, F., Dalimi, A., Shahverdi, A.R., 2013. Efficacy of biogenic selenium nanoparticles against Leishmania major: in vitro and in vivo studies. J. Trace Elem. Med. Biol. 27 (3), 203–207.

Boroumand, S., Safari, M., Shaabani, E., Shirzad, M., Faridi-Majidi, R., 2019. Selenium nanoparticles: synthesis, characterization and study of their cytotoxicity, antioxidant and antibacterial activity. Mater. Res. Express 6 (8), 0850d0858. https://doi.org/10.1088/2053-1591/ab2558.

Chowdhury, N.R., MacGregor-Ramiasa, M., Zilm, P., Majewski, P., Vasilev, K., 2016. 'Chocolate'silver nanoparticles: synthesis, antibacterial activity and cytotoxicity. J. Colloid Interface Sci. 482, 151–158. https://doi.org/10.1016/j.jcis.2016.08.003.

Ebrahimzadeh, M., Hosseinimehr, S., Hamidinia, A., 2008. Antioxidant and free radical scavenging activity of Feijoa sallowiana fruits peel and leaves. Pharmacologyonline 1, 7–14.

Ebrahimzadeh, M.A., Nabavi, S.M., Nabavi, S.F., Eslami, S., 2010. Antioxidant and free radical scavenging activities of culinary-medicinal mushrooms, golden chanterelle Cantharellus cibarius and Angel's wings Pleurotus porrigens. Int. J. Med. Mushrooms 12 (3), 265–272. https://doi.org/10.1615/IntJMedMushr.v12.i3.50.

Elahi, B., Mirzaee, M., Darroudi, M., Oskuee, R.K., Sadri, K., Gholami, L., 2020. Role of oxygen vacancies on photo-catalytic activities of green synthesized ceria nanoparticles in Cydonia oblonga miller seeds extract and evaluation of its cytotoxicity effects. J. Alloys Compd. 816,. https://doi.org/10.1016/j.jallcom.2019.152553 152553.

Eslami, S., Ebrahimzadeh, M.A., Biparva, P., Abedi Rad, M., 2016. Zero valent iron-based nanoparticles: synthesis, characterization and their application in biology and medicine. J. Mazandaran Univ. Med. Sci. 26 (142), 285–310.

Ezhuthupurakkal, P.B., Polaki, L.R., Suyavaran, A., Subastri, A., Sujatha, V., Thirunavukkarasu, C., 2017. Selenium nanoparticles synthesized in aqueous extract of Allium sativum perturbs the structural integrity of Calf thymus DNA through intercalation and

groove binding. Mater. Sci. Eng. C 74, 597–608. https://doi.org/10.1016/j.msec.2017.02.003.

Fardsadegh, B., Vaghari, H., Mohammad-Jafari, R., Najian, Y., Jafarizadeh-Malmiri, H., 2019. Biosynthesis, characterization and antimicrobial activities assessment of fabricated selenium nanoparticles using Pelargonium zonale leaf extract. Green Process. Synth. 8 (1), 191–198. https://doi.org/10.1515/gps-2018-0060.

Faridnia, R., Kalani, H., Fakhar, M., Akhtari, J., 2018. Investigating in vitro anti-leishmanial effects of silibinin and silymarin on Leishmania major. J. Parasitol. Res. 64 (1), 29–35. https://doi.org/10.17420/ap6401.129.

Hamelian, M., Varmira, K., Veisi, H., 2018. Green synthesis and characterizations of gold nanoparticles using Thyme and survey cytotoxic effect, antibacterial and antioxidant potential. J. Photochem. Photobiol. B, Biol. 184, 71–79. https://doi.org/10.1016/j.jphotobiol.2018.05.016.

Hashem, A.H., Abdelaziz, A.M., Askar, A.A., Fouda, H.M., Khalil, A., Abd-Elsalam, K.A., Khaleil, M.M., 2021. Bacillus megaterium-mediated synthesis of selenium nanoparticles and their antifungal activity against Rhizoctonia solani in faba bean plants. J. Fungi 7, 195. https://doi.org/10.3390/jof7030195.

Hashemi, Z., Ebrahimzadeh, M.A., Biparva, P., Mortazavi-Derazkola, S., Goli, H.R., Sadeghian, F., Kardan, M., Rafiei, A., 2020. Biogenic silver and zero-valent iron nanoparticles by feijoa: Biosynthesis, characterization, cytotoxic, antibacterial and antioxidant activities. Anticancer Agents Med. Chem. 20 (14), 1673–1687. https://doi.org/10.2174/1871520620666200619165910.

Hashemi, Z., Mizwari, Z.M., Mohammadi-Aghdam, S., Mortazavi-Derazkola, S., Ebrahimzadeh, M.A., 2022. Sustainable green synthesis of silver nanoparticles using Sambucus ebulus phenolic extract (AgNPs@ SEE): and assessment of photocatalytic degradation of methyl orange and their in vitro antibacterial and anticancer activity. Arab. J. Chem. 15, (1). https://doi.org/10.1016/j.arabjc.2021.103525 103525.

Hassanien, R., Abed-Elmageed, A.A., Husein, D.Z., 2019. Eco-friendly approach to synthesize selenium nanoparticles: photocatalytic degradation of sunset yellow azo dye and anticancer activity. ChemistrySelect 4 (31), 9018–9026. https://doi.org/10.1002/slct.201901267.

Hatami, R., Javadi, A., Jafarizadeh-Malmiri, H., 2020. Effectiveness of six different methods in green synthesis of selenium nanoparticles using propolis extract: screening and characterization. Green Process. Synth. 9 (1), 685–692. https://doi.org/10.1515/gps-2020-0065.

Ismail, A.-W.-A., Sidkey, N.M., Arafa, R.A., Fathy, R.M., El-Batal, A.I., 2016. Evaluation of in vitro antifungal activity of silver and selenium nanoparticles against Alternaria solani caused early blight disease on potato. Biotechnol. J. Int. 1–11. https://doi.org/10.9734/BBJ/2016/24155.

Jay, V., Shafkat, R., 2018. Synthesis of selenium nanoparticles using Allium sativum extract and analysis of their antimicrobial property against gram positive bacteria. Pharma Innov. 7 (9), 262–266.

Keskin, S., Oya, N., Akbal Vural, O., Abaci, S., 2020. Biosynthesis of noble selenium nanoparticles from Lysinibacillus sp. NOSK for antimicrobial, antibiofilm activity, and biocompatibility. Geomicrobiol. J. 37 (10), 919–928. https://doi.org/10.1080/01490451.2020.1799264.

Khalili, M., Fathi, H., Ebrahimzadeh, M.A., 2016. Antioxidant activity of bulbs and aerial parts of Crocus caspius, impact of extraction methods. Pak. J. Pharm. Sci. 29 (3), 773–777.

Kokila, K., Elavarasan, N., Sujatha, V., 2017. Diospyros montana leaf extract-mediated synthesis of selenium nanoparticles and their biological applications. New J. Chem. 41 (15), 7481–7490. https://doi.org/10.1039/C7NJ01124E.

Mahmoudvand, H., Shakibaie, M., Tavakoli, R., Jahanbakhsh, S., Sharifi, I., 2014. In vitro study of leishmanicidal activity of biogenic selenium nanoparticles against Iranian isolate of sensitive and glucantime-resistant Leishmania tropica. Iran. J. Parasitol. 9 (4), 452.

Menon, S., Ks, S.D., Santhiya, R., Rajeshkumar, S., Kumar, V., 2018. Selenium nanoparticles: a potent chemotherapeutic agent and an elucidation of its mechanism. Colloids Surf. B 170, 280–292. https://doi.org/10.1016/j.colsurfb.2018.06.006.

Menon, S., Agarwal, H., Rajeshkumar, S., Rosy, P.J., Shanmugam, V. K., 2020. Investigating the antimicrobial activities of the biosynthesized selenium nanoparticles and its statistical analysis. Bionanoscience 10 (1), 122–135. https://doi.org/10.1007/s12668-019-00710-3.

Menon, S., Agarwal, H., Shanmugam, V.K., 2021. Catalytical degradation of industrial dyes using biosynthesized selenium nanoparticles and evaluating its antimicrobial activities. Sustain. Environ. Res. 31 (1), 1–12. https://doi.org/10.1186/s42834-020-00072-6.

Menon, S., KS, S. D., Agarwal, H., Shanmugam, V. K., 2019. Efficacy of biogenic selenium nanoparticles from an extract of ginger towards evaluation on anti-microbial and anti-oxidant activities. Colloids Interface Sci. Commun. 29, 1-8. https://doi.org/10.1016/j.colcom.2018.12.004.

Mittal, A.K., Kumar, S., Banerjee, U.C., 2014. Quercetin and gallic acid mediated synthesis of bimetallic (silver and selenium) nanoparticles and their antitumor and antimicrobial potential. J. Colloid Interface Sci. 431, 194–199. https://doi.org/10.1016/j.jcis.2014.06.030.

Mortazavi-Derazkola, S., Ebrahimzadeh, M.A., Amiri, O., Goli, H.R., Rafiei, A., Kardan, M., Salavati-Niasari, M., 2020. Facile green synthesis and characterization of Crataegus microphylla extract-capped silver nanoparticles (CME@ Ag-NPs) and its potential antibacterial and anticancer activities against AGS and MCF-7 human cancer cells. J. Alloys Compd. 820,. https://doi.org/10.1016/j.jallcom.2019.153186 153186.

Nabavi, S.F., Nabavi, S.M., Ebrahimzadeh, M.A., Jafari, N., Yazdanpanah, S., 2013. Biological activities of freshwater algae, Spirogyra singularis Nordstedt. J. Aquat. Food Prod. Technol. 22 (1), 58–65. https://doi.org/10.1080/10498850.2011.624292.

Nadaf, N.Y., Kanase, S.S., 2019. Biosynthesis of gold nanoparticles by Bacillus marisflavi and its potential in catalytic dye degradation. Arab. J. Chem. 12 (8), 4806–4814. https://doi.org/10.1016/j.arabjc.2016.09.020.

Nakkala, J.R., Mata, R., Sadras, S.R., 2016. The antioxidant and catalytic activities of green synthesized gold nanoparticles from Piper longum fruit extract. Process Saf. Environ. Prot. 100, 288–294. https://doi.org/10.1016/j.psep.2016.02.007.

Nasrollahzadeh, M., Sajadi, S.M., 2015. Preparation of Au nanoparticles by Anthemis xylopoda flowers aqueous extract and their application for alkyne/aldehyde/amine A 3-type coupling reactions. RSC Adv. 5 (57), 46240–46246. https://doi.org/10.1007/s11164-021-04424-8.

Nasrollahzadeh, M., Sajadi, S.M., Rostami-Vartooni, A., Hussin, S. M., 2016. Green synthesis of CuO nanoparticles using aqueous extract of Thymus vulgaris L. leaves and their catalytic performance for N-arylation of indoles and amines. J. Colloid Interface Sci. 466, 113–119. https://doi.org/10.1016/j.jcis.2015.12.018.

Nguyen, T.H., Vardhanabhuti, B., Lin, M., Mustapha, A., 2017. Antibacterial properties of selenium nanoparticles and their toxicity to Caco-2 cells. Food Control. 77, 17–24. https://doi.org/10.1016/j.foodcont.2017.01.018.

Sabouri, Z., Akbari, A., Hosseini, H.A., Hashemzadeh, A., Darroudi, M., 2019. Bio-based synthesized NiO nanoparticles and evaluation of their cellular toxicity and wastewater treatment effects. J. Mol. Struct. 1191, 101–109. https://doi.org/10.1016/j.molstruc.2019.04.075.

Salem, S.S., Fouda, M.M., Fouda, A., Awad, M.A., Al-Olayan, E.M., Allam, A.A., Shaheen, T.I., 2021. Antibacterial, cytotoxicity and larvicidal activity of green synthesized selenium nanoparticles using

Penicillium corylophilum. J. Clust. Sci. 32 (2), 351–361. https://doi.org/10.1007/s10876-020-01794-8.

Shakibaie, M., Mohazab, N.S., Mousavi, S.A.A., 2015. Antifungal activity of selenium nanoparticles synthesized by Bacillus species Msh-1 against Aspergillus fumigatus and Candida albicans. Jundishapur. J. Microbiol. 8 (9). https://doi.org/10.5812/jjm.26381.

Shirmehenji, R., Javanshir, S., Honarmand, M., 2020. A green approach to the bio-based synthesis of selenium nanoparticles from mining waste. J. Clust. Sci. 1–13. https://doi.org/10.1007/s10876-020-01892-7.

Shirzadi-Ahodashti, M., Mizwari, Z.M., Mohammadi-Aghdam, S., Ahmadi, S., Ebrahimzadeh, M.A., Mortazavi-Derazkola, S., 2022. Optimization and evaluation of anticancer, antifungal, catalytic, and antibacterial activities: biosynthesis of spherical-shaped gold nanoparticles using Pistacia vera hull extract (AuNPs@ PV). Arab. J. Chem. 15,. https://doi.org/10.1016/j.arabjc.2022.104423 104423.

Shokrzadeh, M., Bakhshi Jouybari, H., Talebpour Amiri, F., Ziar, A., Habibpour, P., 2019. Hepatoprotective activity of Caspian saffron (Crocus caspius Fisch and Mey) flowers against CCl4-induced acute liver injury in mice. Res. J. Pharmacogn. 6 (3), 33–39. https://doi.org/10.22127/RJP.2019.89458.

Shubharani, R., Mahesh, M., Yogananda Murthy, V., 2019. Biosynthesis and characterization, antioxidant and antimicrobial activities of selenium nanoparticles from ethanol extract of Bee Propolis. J. Nanomed. Nanotechnol. 10 (1), 1–10. https://doi.org/10.4172/2157-7439.1000522.

Tripathi, R.M., Hameed, P., Rao, R.P., Shrivastava, N., Mittal, J., Mohapatra, S., 2020. Biosynthesis of highly stable fluorescent selenium nanoparticles and the evaluation of their photocatalytic degradation of dye. Bionanoscience 10 (2), 389–396. https://doi.org/10.1007/s12668-020-00718-0.

Vahidi, H., Barabadi, H., Saravanan, M., 2020. Emerging selenium nanoparticles to combat cancer: a systematic review. J. Clust. Sci. 31 (2), 301–309. https://doi.org/10.1007/s10876-019-01671-z.

Vekariya, K.K., Kaur, J., Tikoo, K., 2012. ERα signaling imparts chemotherapeutic selectivity to selenium nanoparticles in breast cancer. Nanomed.: Nanotechnol. Biol. Med. 8 (7), 1125–1132. https://doi.org/10.1016/j.nano.2011.12.003.

Vickers, N.J., 2017. Animal communication: when i'm calling you, will you answer too? Curr. Biol. 27 (14), R713–R715. https://doi.org/10.1016/j.cub.2017.05.064.

Wadhwani, S.A., Shedbalkar, U.U., Singh, R., Chopade, B.A., 2016. Biogenic selenium nanoparticles: current status and future prospects. Appl. Microbiol. Biotechnol. 100 (6), 2555–2566. https://doi.org/10.1007/s00253-016-7300-7.

Wadhwani, S.A., Gorain, M., Banerjee, P., Shedbalkar, U.U., Singh, R., Kundu, G.C., Chopade, B.A., 2017. Green synthesis of selenium nanoparticles using Acinetobacter sp. SW30: optimization, characterization and its anticancer activity in breast cancer cells. Int. J. Nanomed. 12, 6841. https://doi.org/10.2147/IJN.S139212.

Yang, L., Shen, Y., Xie, A., Liang, J., Zhang, B., 2008. Synthesis of Se nanoparticles by using TSA ion and its photocatalytic application for decolorization of cango red under UV irradiation. Mater. Res. Bull. 43 (3), 572–582. https://doi.org/10.1016/j.materresbull.2007.04.012.